Journal of Solid Mechanics Vol. 16, No. 4 (2024) pp. 449-466
DOI: 10.60664/jsm.2024.1130323

Research Paper

Flexural Behavior Assessment of An Eco-Friendly Thermoplastic Composite Sandwich Beam with Recyclable Core and Faces

S.A. Mousavi, H. Shokrollahi *, H. Sabouri

Department of Mechanical Engineering, Kharazmi University, Tehran, Iran

Received 28 August 2024; Received in revised form 26 November 2024; Accepted 6 December 2024

ABSTRACT

This study investigates the flexural behavior of sandwich structures composed of glass fiber-reinforced composite laminates. The cores and matrices of these composites consist of Polyamide (PA), a thermoplastic polymer, which uniquely positions these structures as recyclable options due to their ability to be melted and reused, contributing to sustainable engineering practices. Three-point bending tests were conducted on structures, and the extensive results were thoroughly examined. The sandwich beam cores exhibit three distinct structures: honeycomb, re-entrant auxetic, and sinusoidal ligament. Various parameters were analyzed, including the absorbed energy by the structures, flexural stress on the laminates, shear stress on the cores, and the force-to-weight ratio. Notably, the re-entrant auxetic structure with a 2 mm cell thickness outperformed the other structures in terms of energy absorption and force-to-weight ratio corresponding to failure. The study also highlights that these thermoplastic-based sandwich structures not only offer mechanical benefits but also promote recyclability and potential reuse after end-of-life through remelting processes. The results show that the re-entrant auxetic and honeycomb structures exhibited greater brittleness compared to the sinusoidal ligament structure. Additionally, the sinusoidal ligament structure demonstrated an approximately 10% load increase as the thickness increased from 1.5 to 2 mm. Moreover, the displacement at the point of failure increased by approximately 17% for the sinusoidal ligament and about 30% for the re-entrant auxetic. These recyclable characteristics open new avenues for sustainable applications, where performance and environmental considerations align. These findings contribute valuable insights into the design and optimization of sandwich structures for various engineering applications.

Keywords: Sandwich structure; Recyclable composite; Three-point bending.

*Corresponding author. Tel.: +98 910 2101705.
E-mail address: hshokrollahi@khu.ac.ir (H. Shokrollahi)

.

JOURNAL OF SOLID MECHANICS JSM

Copyright: © 2024 by the authors. Submitted for possible open access publication under the terms and conditions of the Creative Commons Attribution (CC BY) license (https://creativecommons.org/licenses/by/4.0/).

1 INTRODUCTION

SANDWICH panels are significant achievements in the automotive, aerospace, marine, and construction industries [1–3]. These structures typically consist of two faces and an inner layer called the core. They offer excellent sound and thermal isolation properties, exceptional mechanical characteristics relative to weight, high flexural rigidity, and a high strength-to-weight ratio. These qualities distinguish sandwich panels from other structures [4, 5]. The faces of sandwich panels are typically made from metals or composites with good mechanical properties, while the cores can be made from wood, plastic, or foam. One of the core's functions is to fill the space between the two faces [6, 7]. The methods for manufacturing sandwich panels have evolved significantly from the past to the present. Manual layup and casting were older methods for making sandwich panels that have now been replaced by modern techniques such as pre-preg composite, vacuum, hot pressing, and other techniques with less human interference. Contemporary methods result in a higher fiber volume fraction in the composite, leading to improved mechanical properties [8]. Ghorbanpour Arani et al. [9,10] analyzed the nonlinear dynamics of sandwich nanobeams with temperature-sensitive graded cores and magnetostrictive layers, showing that these layers significantly affect displacement and stability through changes in stiffness. In a related study, they examined CNT-reinforced composite microtubes under magnetic fields, finding that magnetic forces and increased CNT content enhance stability and critical fluid velocity. These studies underscore the role of external fields and material composition in optimizing the performance of nanoscale structures.

Cores and faces of sandwich panels can be made from various materials and have different structures, including metals, foams, wood, and fibers. Among the core structures commonly used today, the hexagonal honeycomb structure stands out. This natural pattern enhances mechanical properties while reducing overall weight. Notably, the honeycomb structure also exhibits excellent energy absorption [11]. Another intriguing structure gaining attention is the auxetic structure, which possesses a negative Poisson's ratio. This means it behaves differently under mechanical loads, particularly tension and compression, compared to other structures. When subjected to tension, the auxetic structure expands, while under compression, it narrows [12]. Kurt et al. [13] compared various sandwich structures made from different materials, including balsa wood, aluminum or aramid fibers, and a PVC plastic core. Their study utilized a simple hexagonal honeycomb structure as the core material. Tensile tests revealed that the aluminum alloy with a honeycomb core exhibited higher tensile strength than other structures. In another investigation, Masoumi and Rahimi [14] explored the effect of geometric shape on the flexural behavior of curved composite-faced sandwich panels with a cellular core. They considered two core structures: square and isogrid. Experimental testing demonstrated that the isogrid core exhibited 12% higher flexural stiffness than a similar sample with a square core. Numerical simulations supported this finding, showing a 2% higher flexural stiffness for the isogrid core. Ebrahimi et al. [15] studied a composite structure reinforced with carbon nanotubes under uniform bending loads. They observed that flexural deformation increased with auxetic beam porosity. Additionally, a re-entrant lattice helped control system deflection. Indreș et al. [16] compared different auxetic topologies used in sandwich panel cores subjected to a three-point bending test. All the cores were produced using 3D printing technology. Their experiment included honeycomb, re-entrant auxetic, and chiral topologies. Using the Fused Deposition Modeling (FDM) method, the sandwich beam was manufactured from Polylactic acid (PLA) material. The results showed that the chiral core exhibited lower strength than the honeycomb core, making these topologies particularly suitable for applications requiring high stiffness.

The increasing focus on sustainability in material design has led to the development of eco-friendly sandwich panels using recyclable core and faces. The use of thermoplastic composite materials offers a promising alternative to traditional sandwich panels, providing both environmental benefits and mechanical performance [17–20]. Studies have investigated the use of recycled polyethylene terephthalate (r-PET) plastic as a core component, combined with bio-based polymer resin and continuous PET fibers for the facing component Studies have investigated the use of r-PET plastic as a core component, combined with bio-based polymer resin and continuous PET fibers for the facing component [21,22]. Additionally, the incorporation of recycled flax/bio-based epoxy composite cores and skins in sandwich panels has shown promising results, with panels made of 4 mm recyclates exhibiting superior mechanical properties [21]. Furthermore, the natural frequencies of sandwich panels with laminate faces have been analyzed, showing that design parameters such as panel length, core thickness, and fiber-reinforced angle significantly impact the vibration response [23]. Moreover, Beigpour et al. [24,25] worked on natural fibers such as kenaf and cotton. These fibers possess high mechanical qualities, making them widely used in polymer composite laminates with natural fibers. A dissolved chloroform and polylactic acid mixture was used as the matrix material. Three-point bending and tensile tests were conducted, and the Finite Element Method (FEM) was utilized to validate the results. The findings showed that by doubling the thickness of the composite and halving it, the force increased by about 660% and decreased by about 87%, respectively. Chung et al. [26] conducted a study on the shear stiffness and

energy absorption of an auxetic open-cell foam used as a sandwich core material. Polyurethane (PU) was used in this experiment. Thermoformed auxetic foams were employed in sandwich beams with carbon fiber/epoxy faces. The results indicate that the auxetic foam exhibits a shear modulus 7% lower than that of the bulk specimen but demonstrates higher shear stress under large deformations. Kaboğlu [27] incorporated PA12 (Nylon 12) and GFRPP (Glass Fiber Reinforced Polypropylene) as strengthening materials in the top and bottom layers of a structure designed specifically for automobile bumpers. The core structure of the sandwich panels was produced using the Fused Deposition Modeling (FDM) method. Subsequently, a three-point bending test was performed on two sets of samples, with the primary distinction between the two sets being the cell length and thickness. The outcomes revealed that the first group exhibited a higher load-bearing capacity. In a much broader study, Harizi et al. [28] investigated the mechanical properties of carbon fiber-reinforced composite sandwich panels under three-point bending. The difference between their work and this paper lies in the use of glass fibers in the faces and the use of newer and more used structures like auxetic structures in cores. For examining flexural behavior, they utilized a three-point bending test using a mechanical-acoustic experimental coupling approach. A novel method has been employed to assess momentary damage in the structure. The material used in this study is Nomex, aluminum and PEI, and structures used in cores are honeycomb, straight tubular and inclined tubular. While sandwich panels made of aluminum showed the highest stiffness, PEI absorbed the highest energy and exhibited higher ductility.

This study aims to assess the flexural behavior of a thermoplastic composite sandwich beam with a recyclable core and faces, contributing to the growing body of knowledge on sustainable materials for structural applications. Despite extensive research in related areas, there remains a gap in specific topics. This study focuses on modifying core materials and core geometry, which are extensive research areas in themselves. Therefore, it is relevant to investigate auxetic structures with thermoplastic materials in sandwich beams and compare their flexural behavior. Additionally, the honeycomb structure has been introduced to provide a comparative basis and enhance our understanding of auxetic structure performance. Displacement, energy absorption, and the force-to-weight ratio are among the aspects that will be investigated and compared for thermoplastic sandwich structures.

2 METHODOLOGY AND EXPERIMENTS

The motivation of this work is to propose a lightweight sandwich structure that is to a certain extent recyclable or repairable and has significant load-carrying capability. Due to the considerable increase in the use of sandwich structures across various industries, if recycling and repair issues are not addressed, the environmental impact originating from the accumulation of plastics will be faced by mankind.

Based on the previous research reviewed in the introduction, the current study has been concerned with the flexural behavior of a recyclable composite sandwich structure. With these prerequisites, polyamide, which is a thermoplastic material with moderate mechanical properties, has been chosen as the base material for the sandwich structure. The core has been made from polyamide, and the facing plates of the sandwich structure have been manufactured using a glass/polyamide composite. Based on these considerations, the thermoplastic material could be recycled. Additionally, the structure could be repaired via local heating.

E-glass fiber fabrics possessing an areal density of 300 gr/m² and a polyamide film with a thickness of 500 microns have been used for manufacturing the facing plates of the sandwich structure. The facing plates consist of 4 layers of fibers and 3 layers of resin film. The composite has been manufactured into a steel frame with dimensions of 220 mm × 220 mm × 1 mm, using a hot press machine (Fig. 1). The temperature of the press and the duration of manufacturing have been set to 240 degrees Celsius and 45 minutes, respectively. The resulting composite laminate has a thickness of 1 mm and an approximate fiber volume fraction of 40%.

Fig. 1
Hot press machine.

As mentioned before, three different geometries have been considered for the core structure of the sandwich beam. One of the geometries is the well-known hexagonal honeycomb structure, another is a re-entrant auxetic shape, and the third is a sinusoidal ligament shape. The cell wall thicknesses vary between 1.5, 2, and 2.5 millimeters. The dimensions of the structures and cores are calculated, designed, and constructed by the ASTM C393. The cores have been manufactured on an 8 mm thickness of a polyamide sheet, using a CNC milling machine.

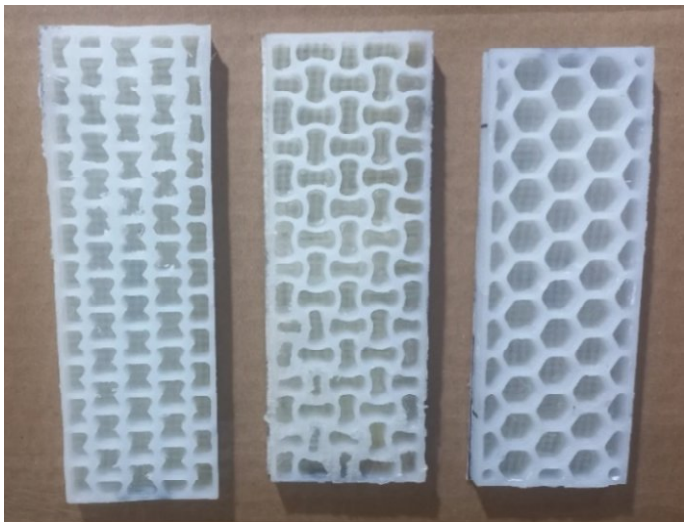

(a) (b) (c)

Fig. 2
Specimens (sandwich cores) prepared for mechanical testing; (a) re-entrant auxetic, (b) sinusoidal ligament, (c) honeycomb.

According to the literature review of cutting all grades of polyamide materials, employing a cooling system for high-speed machining has been recommended. In the absence of a cooling system, reducing the rotational speed of the spindle and feed rate to prevent overheating has also been recommended. Since the cooling system is not employed for machining operations of the cores, the rotational speed of the cutting tool has been set to 8000 rpm. Fig. 2 represents three structures that have undergone experimentation and examination. The specimens include the honeycomb, the sinusoidal ligament, and the re-entrant auxetic structures.

Besides, the bonding between the core and faces has been established using cyanoacrylate adhesive. For bonding between each side of the core and facing plates, less than 5 grams of the adhesive have been consumed. After using the adhesive, the samples were placed under pressure for 16 hours, followed by an additional 16 hours for the adhesive to dry. During the second 16-hour period, no additional pressure was applied, resulting in a more stable and better-formed bond.

A total of 27 samples have been tested, grouped into 9 main categories, with 3 samples from each category used to validate the results. These 9 main categories consist of three different structures and three thicknesses. Table 1 provides their numbering along with some basic properties. The initial letter (A, B, or C) indicates the type of core, where A corresponds to a honeycomb core, B to a re-entrant auxetic core, and C to a sinusoidal ligament core. The first digit after the letter specifies the core thickness: 0 represents a thickness of 1.5 mm, 1 indicates 2 mm, and 2 denotes 2.5 mm. The second digit is an index (0, 1, or 2) used to label repeated tests with the same core type and thickness. These categories vary in structure and core thickness, allowing for a comprehensive examination of their properties and performance.

The three-point bending test was conducted according to ASTM C393, and all standard procedures were followed. Additionally, for the composite samples, a tensile test was performed according to ASTM D3039 to better understand the mechanical properties and facilitate numerical simulations. The loading rates were set to 2 millimeters per minute for the tensile test of composite samples and 3 millimeters per minute for the structures under three-point bending test. Fig. 3 shows a sample under a three-point bending test at the moment of failure.

Table 1
Dimensional properties of the sandwich beam samples

Samples Code	Core type; Cell wall thickness (mm)	Core Weight (g)	Faces Weight (g)	Total weight (g)	Thickness (mm)	Width (mm)	Length (mm)
A0	Honeycomb; 1.5	25.40	17.70	60.80	10.8	52	154
A1	Honeycomb; 2	29.63	19.05	67.73	10.8	52	154
A2	Honeycomb; 2.5	38.57	20.05	77.67	10.8	52	154
B0	Re-entrant auxetic; 1.5	37.11	20.04	77.19	10.8	52	167
B1	Re-entrant auxetic; 2	45.45	18.67	82.79	10.8	52	167
B2	Re-entrant auxetic; 2.5	49.35	19.60	88.55	10.8	52	167
C0	Sinusoidal ligament; 1.5	32.01	20.08	72.17	10.8	52	158
C1	Sinusoidal ligament; 2	42.23	18.35	78.93	10.8	52	158
C2	Sinusoidal ligament; 2.5	47.24	20.50	88.24	10.8	52	158

Fig. 3
Sandwich beam sample under a three-point bending test.

Figs. 4 and 5 are related to composite samples and stress diagrams used for the tensile test. Numerical simulations were conducted by inputting the elastic modulus of the polyamide region and the fiber volume fraction to compare the results with experimental test data. Table 2 shows the elastic modulus calculated from the experimental test for all samples.

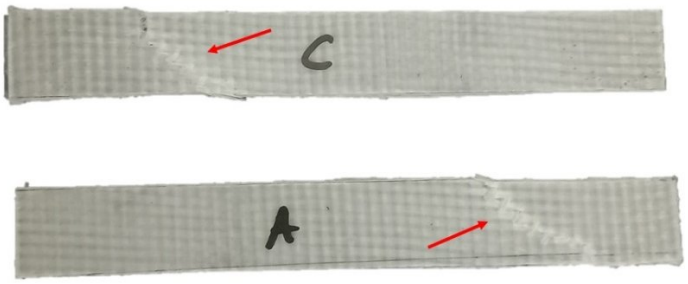

Fig. 4
Composite samples after failure.

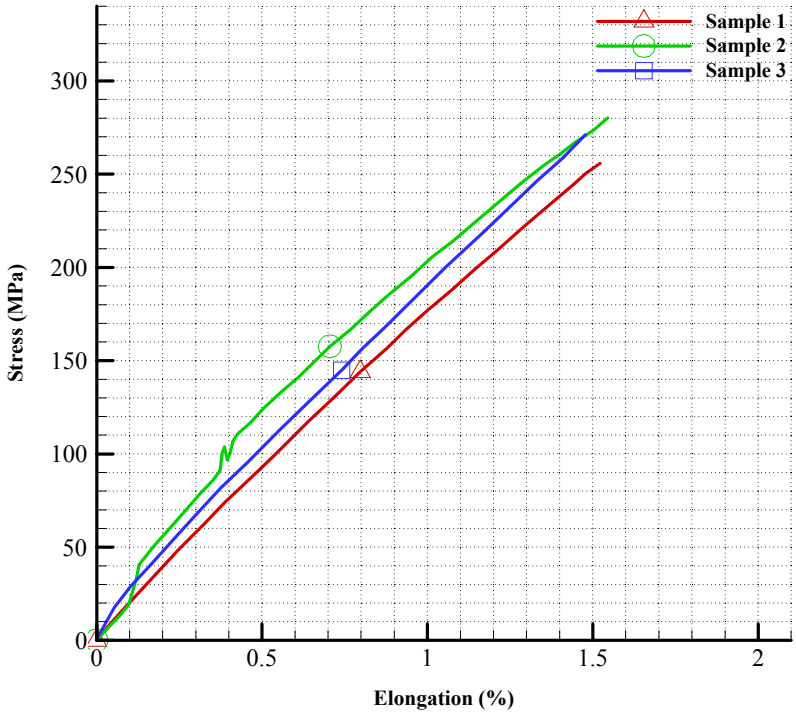

Fig. 5
Stress-elongation diagram for tensile test of composite samples.

Table 2
Elastic modulus for composite samples

	Elastic Modulus (GPa)
Sample 1	14.6
Sample 2	16.2
Sample 3	15.8
Mean	15.5

Moreover, a numerical analysis has been conducted to compare the results of tensile testing on the composite specimen, and the load-deflection diagram is shown in Fig. 6. The proximity of the numerical and experimental outcomes demonstrates the precision of the conducted tests. The discrepancy between the numerical and experimental analyses observed at displacements greater than 0.2 mm is attributed to defects during the manufacturing process and the linear nature of the numerical modeling. In the numerical model, plasticity and non-elastic deformations were not considered, and the structure was modeled as defect-free, leading to slight differences in behavior. Regarding the step behavior observed in the curve of sample B, the cause is attributed to friction and stick-slip effects.

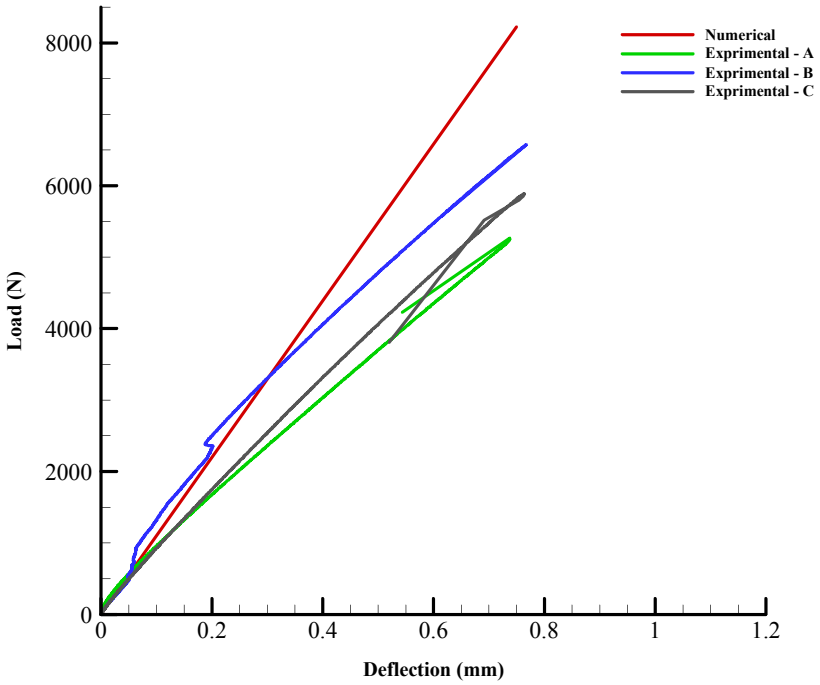

Fig. 6
Load-deflection curve for numerical and experimental analysis for composite samples.

3 EXPERIMENTAL RESULTS

Initially, different structures with uniform cell wall thickness were compared. Load-deflection diagrams were plotted for all three structures and one thickness within the same frame. The simple honeycomb structure had the lowest load-bearing capacity, while the re-entrant auxetic structure had the highest. The same approach was followed for other thicknesses, except that sample B2 experienced defects during the construction phases. During the bending test, the primary mode of failure shifted from the faces and core to the separation between the skin and core. This alteration significantly affected the load-bearing behavior of the structure in terms of how much weight it could carry. Fig. 7 shows a sample under a three-point bending test at the moment of failure. Figs. 8 and 9 show the load-deflection diagram for comparing samples with the same cell thicknesses and different core structures. Note that the presented results represent average values for each sample category.

Fig. 7
Sandwich beam sample under a three-point bending test at the moment of failure.

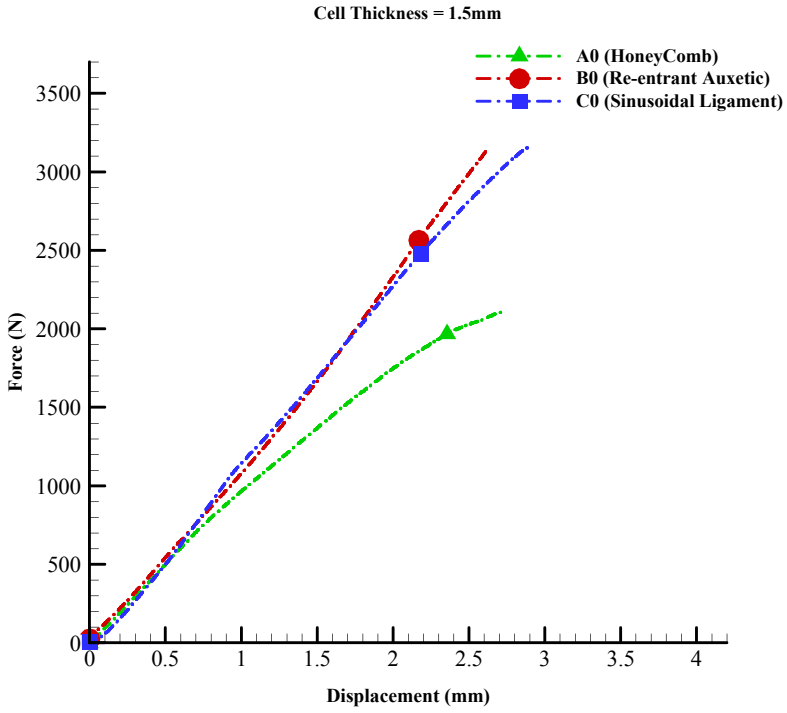

Fig. 8
Load-deflection diagram for sandwich beam samples having 1.5 mm cell thickness core.

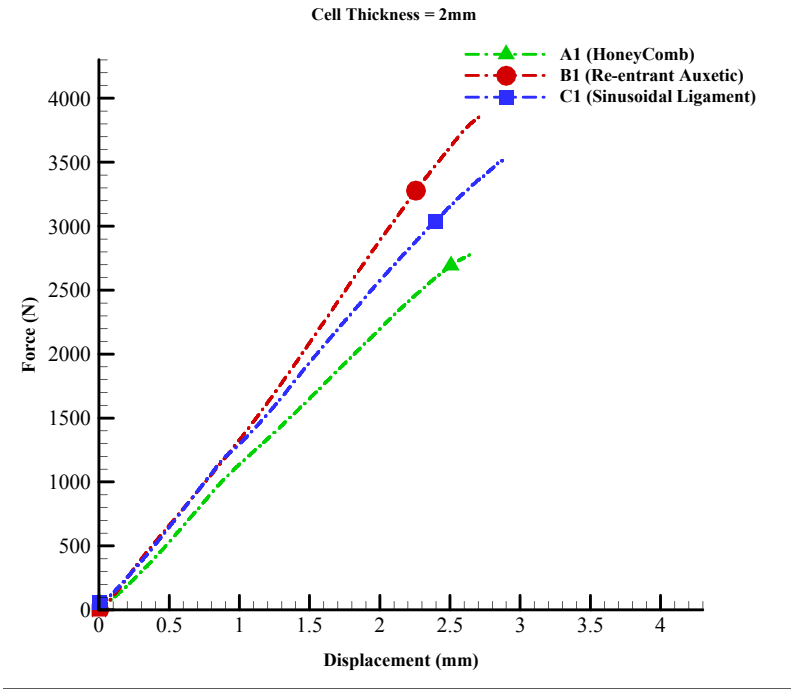

(a)

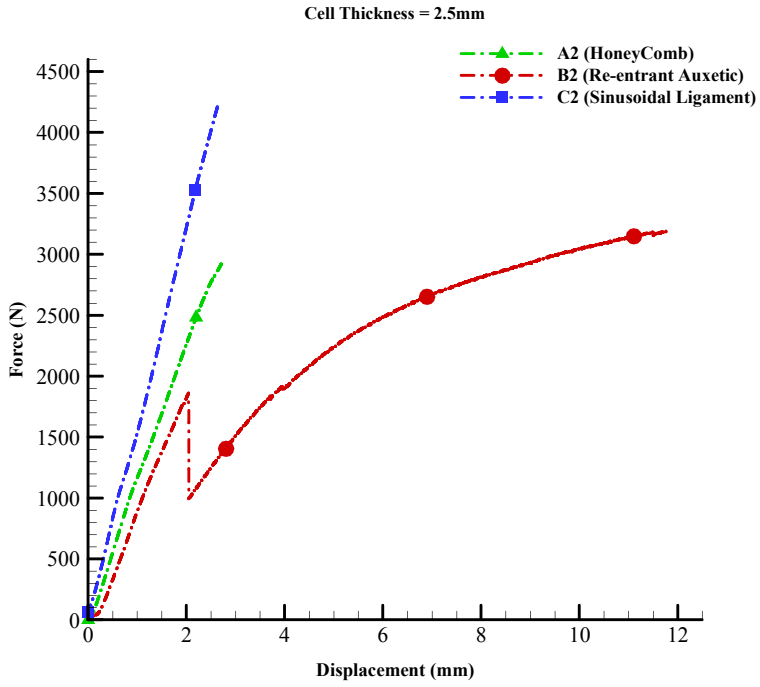

(b)

Fig. 9
Load-deflection diagram for sandwich beam samples having 2 mm (a), and 2.5 mm (b) cell thickness cores.

This analysis highlights the importance of the structure's integrity and the bond quality between the faces and core, which can profoundly impact its load-bearing capacity.

Notably, the samples C11 (1st sample of C1 category) and B12 (2nd sample of B1 category) are compared. Both structures have a cell wall thickness of 2 millimeters, but one has a sinusoidal ligament structure (C12), while the other is a re-entrant auxetic structure (B12). Based on the load-deflection diagram shown in Fig. 9 it can be concluded that the re-entrant auxetic structure (B12) is more brittle compared to the sinusoidal ligament structure (C11). This is evident because it experienced final failure at lower displacements, indicating a lower ductility than the sinusoidal ligament structure. Similar conclusions hold for other thicknesses. Moreover, as shown in Fig. 9(b), a local failure occurred in the re-entrant auxetic structure. However, to reach a better conclusion, it is necessary to examine the complete diagram from beginning to end, representing the final failure of the samples. These comprehensive results are presented in the diagrams of Fig. 10. In Fig. 10, in addition to the load-deflection diagram for a thickness of 2 millimeters, diagrams for a thickness of 1.5 millimeters are also plotted. As observed, the sinusoidal ligament specimen experiences more displacement before failure compared to the re-entrant auxetic specimen.

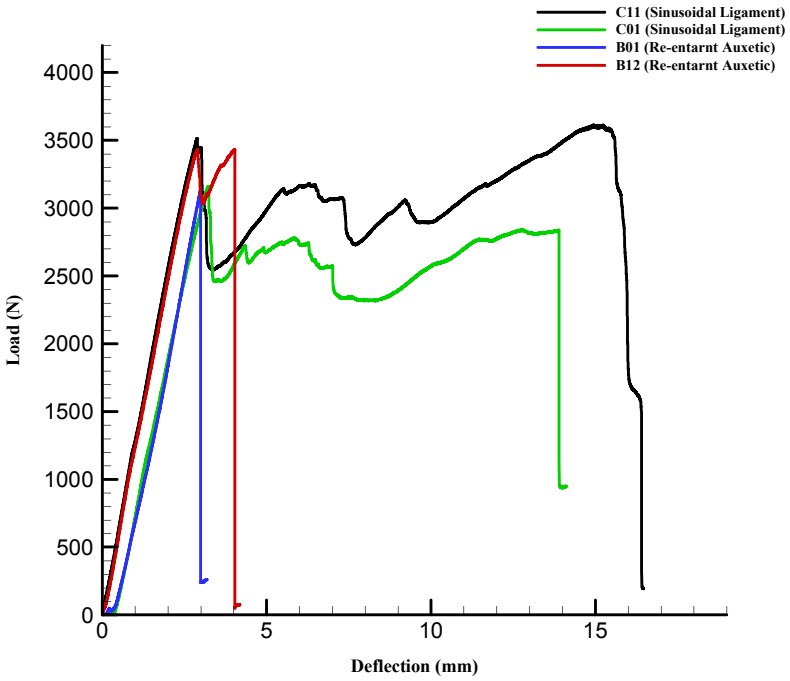

Fig. 10
Comparison of the load-deflection diagram for C1, B1, C0, and B0 sandwich beam samples.

As shown in Fig. 10, the sinusoidal ligament specimen exhibits greater toughness compared to the re-entrant auxetic specimen. This is primarily due to the geometry of the core and the orientation of the cells. Additionally, the curvilinear shape of the sinusoidal ligament specimen contributes to its superior performance relative to the re-entrant auxetic specimen.

To gain a more comprehensive understanding of the behavior of different samples, shear forces have been analyzed. Table 3 provides data on the force and core shear stress corresponded to failure, and Fig. 11 displays the normalized force-to-weight ratio corresponded to failure.

Table 3
Force and core shear stress corresponded to failure, for sandwich beam samples

	Core Shear Stress (MPa)	Force Corresponded to Failure (N)
A0	2.25	2257
A1	2.50	2504
A2	3.04	3050
B0	2.94	2949
B1	3.76	3770
B2	1.81	1816
C0	2.79	2800
C1	3.44	3450
C2	3.86	3875

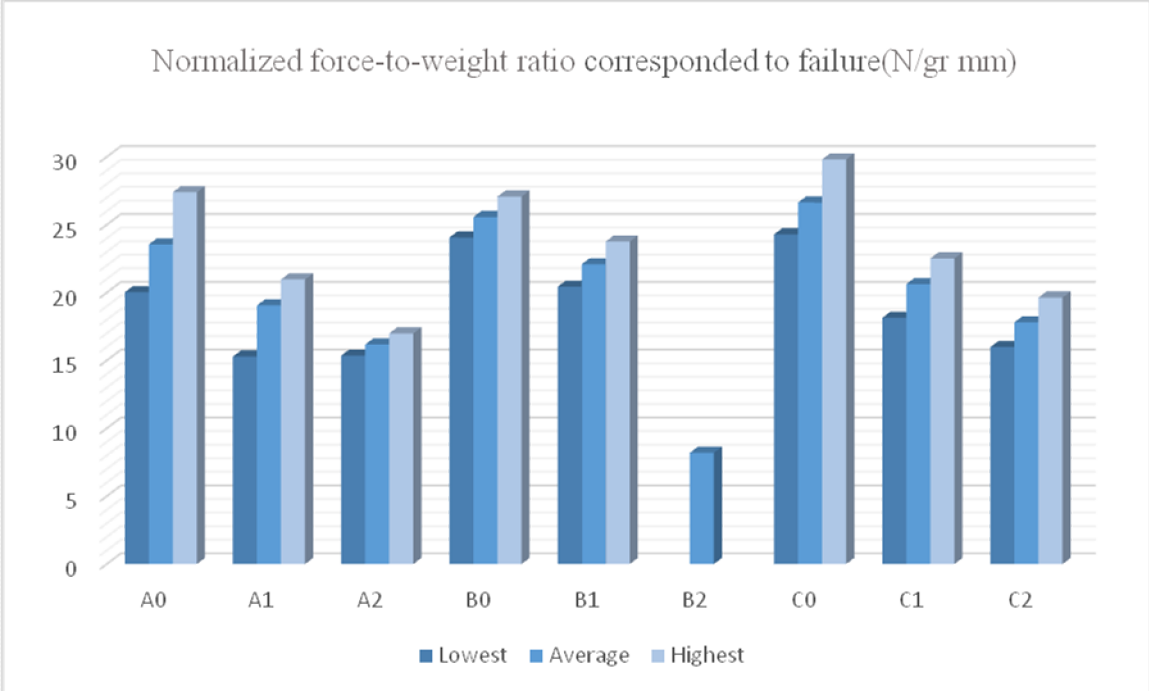

Fig. 11
Normalized force-to-weight ratio corresponded to failure for different sandwich beam samples.

Fig. 12 shows the normalized energy absorption per cell wall thickness for each sample. Re-entrant auxetic and sinusoidal ligament structures with 2- and 1.5-mm thickness have the highest amount of absorbed energy. Additionally, Fig. 11 indicates that thinner thicknesses are associated with the best force-to-weight ratio. It is important to note that during sample preparation, errors occurred in the B2 category. Consequently, out of the three prepared samples, only one is used for the final report. Unfortunately, due to practical constraints, additional samples cannot be prepared for this category. As a result, the maximum and minimum values are not presented. However, considering the overall trend observed in other samples, there is a possibility that the results from this category may not be entirely reliable.

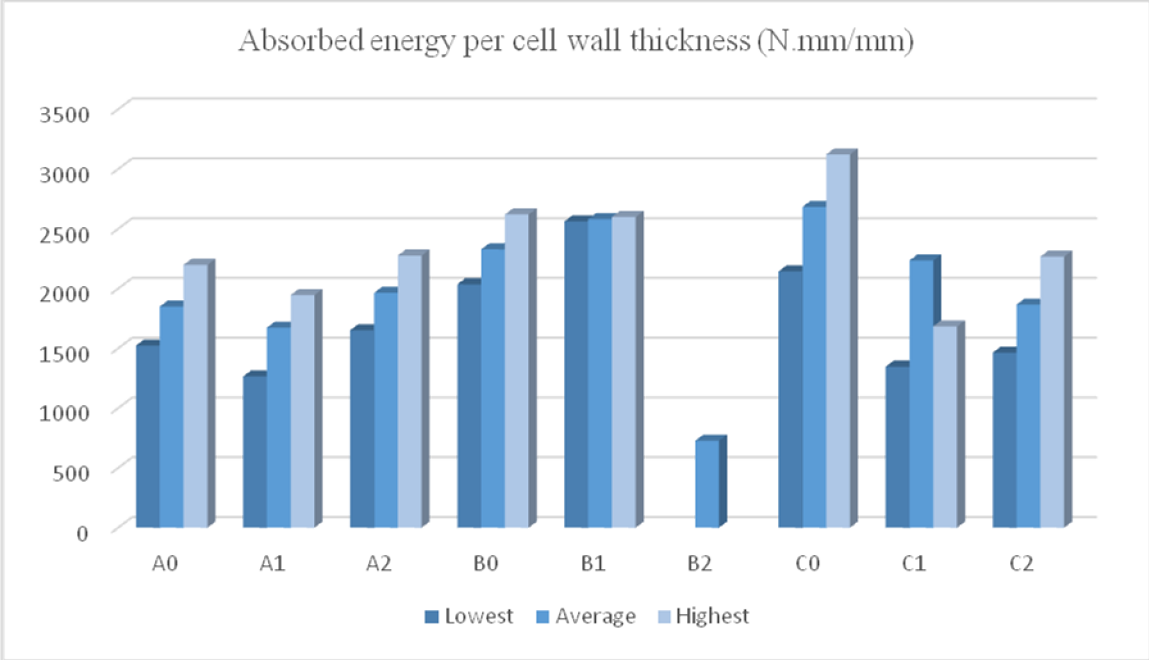

Fig. 12
Energy absorption during three-point bending test for different sandwich beam samples.

It should be noted that, the values presented in Figs. 11 and 12 have been normalized with respect to the thickness of the cell walls, while for Fig. 13, normalization is based on the sample weight. In addition to the average value, which serves as a reference, the minimum and maximum values have also been provided. As displayed in Fig. 12, increased cell wall thickness decreases the absorbed energy in the honeycomb samples. However, the re-entrant auxetic structure shows the opposite trend. Interestingly, the sinusoidal ligament structure behaves similarly to the honeycomb structure. This comparison has been conducted for all samples, specifically in the elastic region. Increasing cell wall thickness naturally results in a heavier core and structure. Consequently, it is expected that thicker structures can bear more load. On the other hand, Fig. 13 reveals a different trend. Excluding B2 samples, thicker thicknesses in honeycomb and re-entrant auxetic structures are associated with better energy-to-weight ratios. For sinusoidal ligament structures, thinner thicknesses perform best.

The choice of structure thickness depends on specific performance requirements: whether optimizing for energy absorption or force-to-weight ratio. Re-entrant auxetic and sinusoidal ligament structures show promise for energy absorption, while honeycomb structures favor energy-to-weight efficiency. Ultimately, the force-to-weight ratio serves as a valuable criterion for comparing different structures and thicknesses in terms of their load-bearing capacity, helping identify the most suitable structure with the highest force-to-weight ratio.

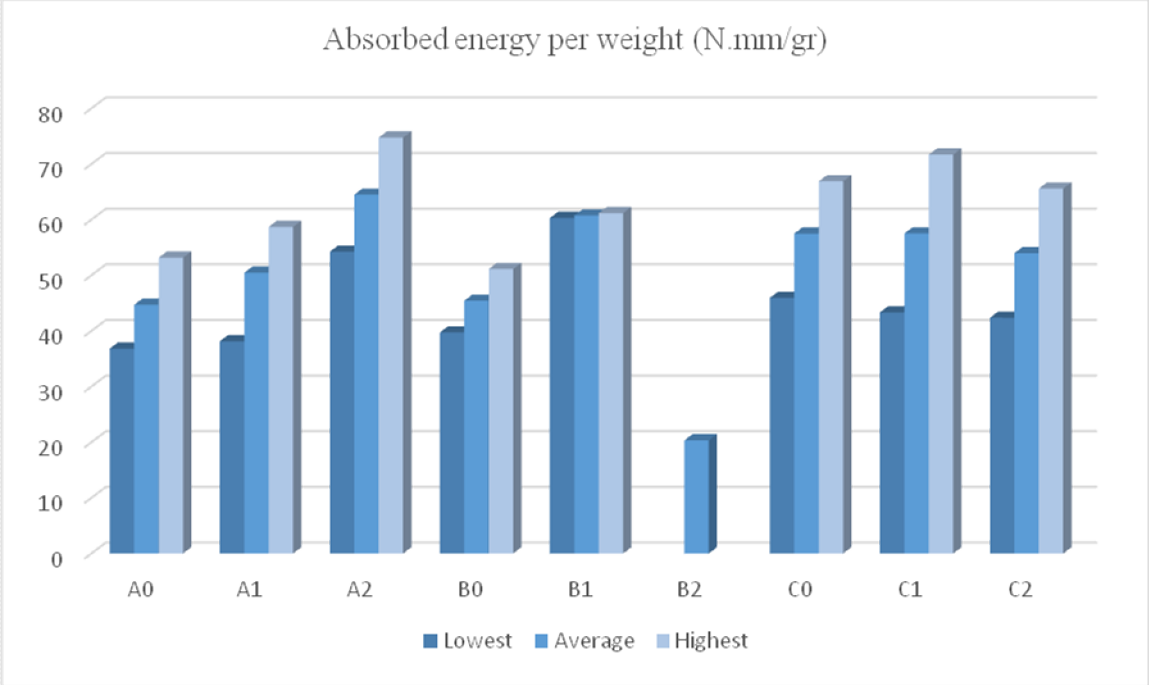

Fig. 13
Normalized absorbed energy during three-point bending test for different sandwich beam samples.

Based on the plotted diagrams, it is observed that samples B1 and C0 exhibit a relatively significant difference compared to other structures and thicknesses. This indicates the enhanced efficiency of a 2-millimeter thickness for the re-entrant auxetic structure and a 1.5-millimeter thickness for the sinusoidal ligament structure. Furthermore, the sinusoidal structure demonstrates the highest force-to-weight ratio. This suggests that the sinusoidal ligament structure might be preferable if a more flexible structure is required. For sinusoidal ligaments, the load increases by approximately 10% when the thickness is raised from 1.5 to 2 millimeters. Additionally, the displacement at the point of failure rises by around 17% for the sinusoidal ligament. In the case of the re-entrant auxetic, the loading level also experiences an increase of about 10% as the thickness changes from 1.5 to 2 millimeters. Moreover, the displacement up to the point of failure shows a rise of approximately 30% for the re-entrant auxetic structure. Considering the absorbed energy relative to cell wall thickness and the energy absorption per weight ratio, it can be concluded that the sinusoidal ligament structure demonstrates superior performance. Additionally, this structure has also shown better results in terms of the force-to-weight ratio at the point of failure.

To investigate the behavior of different structures failure modes, a study was conducted. As shown in Fig. 14, the failure modes included core failure, debonding between the core and face, face failure, and face crushing.

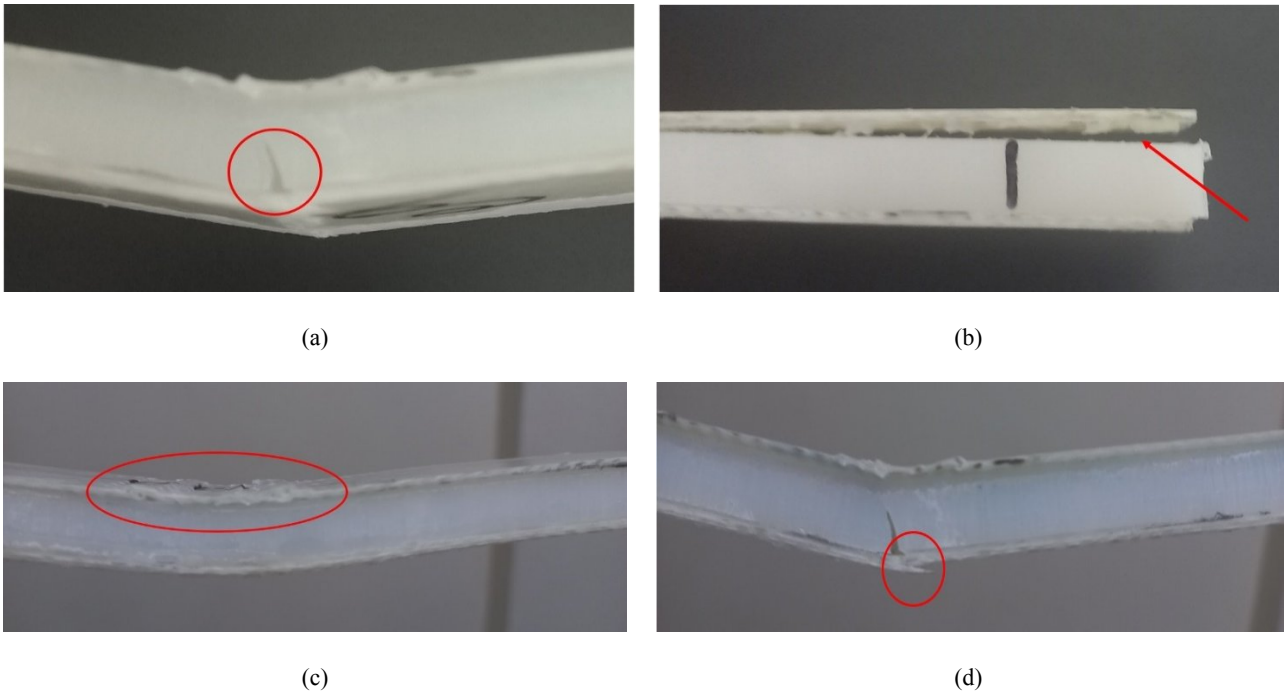

Fig. 14
Different failure modes of sandwich beam samples; (a) core failure, (b) debonding between core and face, (c) face crushing, and (d) face failure.

Fig. 14(a) illustrates that the core of the sandwich beam failed under loading, making core failure the primary mode in the structure. In Fig. 14(c), the crushing of the upper layer is evident, but in composite structures, the main failure mode is typically not layer crushing. Even after crushing, the structure's load-bearing capacity does not decrease significantly. Fig. 14(d) shows a face that has broken and completely separated due to loading, with torn fibers. Ideally, when the structure can bear the highest load, multiple failure modes occur simultaneously. However, when this doesn't happen, usually more than one failure mode renders the structure unable to bear the load. Multiple failure modes are common in each structure, as observed in Fig. 14. It should be noted that the crushing in Fig. 14(c) is due to compressive load, while the failure in Fig. 14(d) occurred due to tensile load.
Based on tests and investigations, the main failure modes for different samples were as follows:

- For the honeycomb samples (A series), core failure was the primary mode. After core plasticization, crushing was also observed in the faces, although the faces rarely failed completely.
- For the sinusoidal ligament samples (B series), core failure remained the main mode. Compared to A samples, more plastic deformation occurred in the core, and local damage was observed in the faces.
- For the re-entrant auxetic samples (C series), multiple failure modes occurred simultaneously. In C0 and C1 samples, core failure, changes in plastic failure in the faces and core, and crushing in the faces were observed. In sample C1, core and face failure occurred simultaneously, with prior crushing of the faces and plastic deformation of the core.

In Fig. 10, the curve changes after reaching the plastic region, exhibiting a different growth trajectory. Initially, force decreases with increasing displacement, but then it rises again. Sometimes, the force even exceeds its previous values. This non-linear and oscillatory behavior relates to the material structure. When the core breaks or enters the plastic region during flexural loading, compressed portions above the neutral axis continue to compress, resulting in densification between cell walls. This densification allows the structure to bear greater loads. The cyclic process of cell wall rupture and compaction continues until another failure mode occurs.

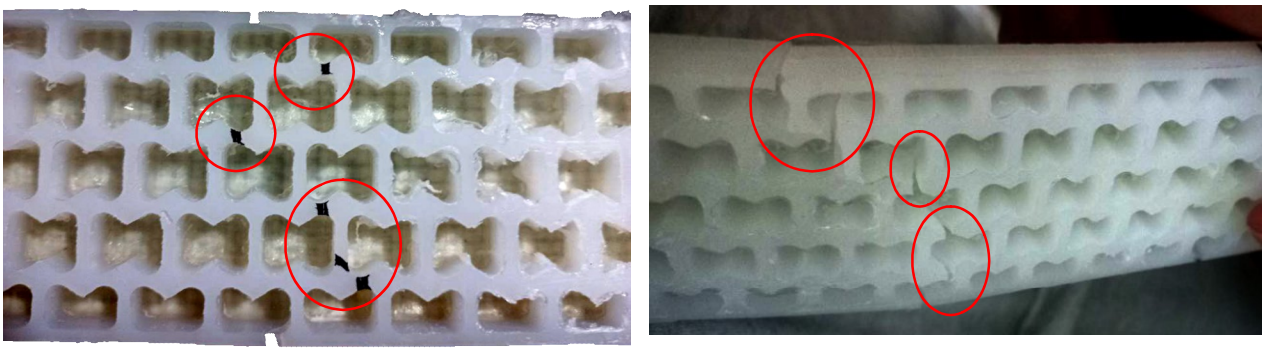

(a) (b)

Fig. 15
The core of sandwich beam sample A22 after three-point bending test.

To better understand the core failure modes, after mechanical tests, the faces and cores of several samples were separated. For example, in Fig. 15, the fracture path within the core of sample A22 is indicated. Fig. 15(a) marks the fracture path, while Fig. 15(b) shows clearly separated regions. The fracture path predominantly occurs at the loading location with the highest displacement. Each sample's distinct core structure may exhibit a different fracture path due to manufacturing defects. If the thickness of cell walls changes slightly during cutting, the fracture path will shift toward the weaker-walled cells. Note that the core failure is mainly due to shear effects, which result in shear forces exceeding the shear strength of the sandwich beam core.

4 CONCLUSION

In this study, sandwich structures with an approximate thickness of 10 millimeters were analyzed. These structures consist of a core and two composite faces. The composite faces are composed of glass fibers and thermoplastic polyamide resin, each with a thickness of approximately 1 millimeter. The cores are also made of polyamide, with an approximate thickness of 8 millimeters. Three distinct structural configurations were investigated and tested.
The results revealed important insights. First, the re-entrant auxetic structure, characterized by a 2-millimeter cell thickness, exhibited a superior force-to-weight ratio compared to the other structures and thicknesses, highlighting its potential for applications where lightweight yet strong materials are essential. Second, the sinusoidal ligament structure demonstrated higher ratios, indicating that the simple hexagonal honeycomb structure is comparatively weaker and less suitable. The notable performance of the sinusoidal ligament structure, particularly in terms of energy absorption and force-to-weight ratio, suggests its potential for use in engineering applications where higher energy dissipation is needed. Particularly, the sinusoidal ligament structure exhibited greater displacement before ultimate failure, suggesting relative ductility which is advantageous for structures that require resilience under loading conditions. Furthermore, the simple hexagonal honeycomb structure displayed weaker energy absorption and force-to-weight ratio performance during the three-point bending test, emphasizing its inferior bending behavior among the three investigated structures.

Drawing from previous research and the findings of this study, several avenues for future investigation are proposed. Researchers should explore the evaluation of Poisson's ratio in recyclable core materials with auxetic structures and examine the tensile behavior of recyclable composite sandwich structures.

REFERENCES

[1] R. Kassab and P. Sadeghian, *Three-Point Bending of Sandwich Beams with FRP Facing and PP Honeycomb Core*, vol. 239. Springer Nature Singapore, 2023.

[2] M. He and W. Hu, "A study on composite honeycomb sandwich panel structure," *Mater. Des.*, vol. 29, no. 3, pp. 709–713, 2008, doi: 10.1016/j.matdes.2007.03.003.

[3] B. R. Noton, "Honeycomb Sandwich Construction for Supersonic Aircraft," *Aircr. Eng. Aerosp. Technol.*, vol. 29, no. 1, pp. 13–18, 1957, doi: 10.1108/eb032782.

[4] J. Grünewald, P. Parlevliet, and V. Altstädt, "Manufacturing of thermoplastic composite sandwich structures: A review of literature," *J. Thermoplast. Compos. Mater.*, vol. 30, no. 4, pp. 437–464, 2017, doi: 10.1177/0892705715604681.

[5] S. Cheng, W. Yu, X. Zhao, Y. Xin, and X. Liu, "Flexural behavior of composite sandwich panel of aluminum foam and epoxy resin," *Emerg. Mater. Res.*, vol. 6, no. 2, pp. 276–284, 2017, doi: 10.1680/jemmr.16.00123.

[6] D. Way, A. Sinha, F. A. Kamke, and J. S. Fujii, "Evaluation of a Wood-Strand Molded Core Sandwich Panel," *J. Mater. Civ. Eng.*, vol. 28, no. 9, pp. 1–9, 2016, doi: 10.1061/(asce)mt.1943-5533.0001589.

[7] S. Dinesh, T. Rajasekaran, M. Dhanasekaran, and K. Vigneshwaran, "Experimental testing on mechanical properties of sandwich structured carbon fibers reinforced composites," *IOP Conf. Ser. Mater. Sci. Eng.*, vol. 402, no. 1, 2018, doi: 10.1088/1757-899X/402/1/012180.

[8] E. A. Franco-Urquiza *et al.*, "Innovation in aircraft cabin interior panels part i: Technical assessment on replacing the honeycomb with structural foams and evaluation of optimal curing of prepreg fiberglass," *Polymers (Basel).*, vol. 13, no. 19, 2021, doi: 10.3390/polym13193207.

[9] A. H. Ghorbanpour-Arani, M. Abdollahian, and A. Ghorbanpour Arani, "Nonlinear dynamic analysis of temperature-dependent functionally graded magnetostrictive sandwich nanobeams using different beam theories," *J. Brazilian Soc. Mech. Sci. Eng.*, vol. 42, no. 6, 2020, doi: 10.1007/s40430-020-02400-8.

[10] A. Ghorbanpour Arani, E. Haghparast, and A. H. Ghorbanpour Arani, "Size-dependent vibration of double-bonded carbon nanotube-reinforced composite microtubes conveying fluid under longitudinal magnetic field," *Polym. Compos.*, vol. 37, no. 5, pp. 1375–1383, May 2016, doi: https://doi.org/10.1002/pc.23306.

[11] A. B. H. Kueh and Y. Y. Siaw, "Impact resistance of bio-inspired sandwich beam with side-arched and honeycomb dual-core," *Compos. Struct.*, vol. 275, no. July, p. 114439, 2021, doi: 10.1016/j.compstruct.2021.114439.

[12] Y. Hou, Y. H. Tai, C. Lira, F. Scarpa, J. R. Yates, and B. Gu, "The bending and failure of sandwich structures with auxetic gradient cellular cores," *Compos. Part A Appl. Sci. Manuf.*, vol. 49, pp. 119–131, 2013, doi: 10.1016/j.compositesa.2013.02.007.

[13] K. A. Feichtinger, "Test Methods and Performance of Structural Core Materials -1. Static Properties," *J. Reinf. Plast. Compos.*, vol. 8, no. 4, pp. 334–357, 1989, doi: 10.1177/073168448900800402.

[14] S. Masoumiasl and G. Rahimi, "Experimental and numerical investigation of effect of shape of ribs on flexural behavior of curved composite sandwich panels with lattice core under," *J. Sci. Technol. Compos.*, vol. 6, no. 3, pp. 351–362, 2019, [Online]. Available: http://jstc.iust.ac.ir/article_34591.html%0Ahttp://jstc.iust.ac.ir/article_34591_0c18d896837d07cf1fa5555aec229795.pdf.

[15] F. Ebrahimi and A. Dabbagh, "Porosity Effects on Static Performance of Carbon Nanotube-Reinforced Meta-Nanocomposite Structures," *Micromachines*, vol. 14, no. 7, 2023, doi: 10.3390/mi14071402.

[16] A. I. Indreș, D. M. Constantinescu, and O. A. Mocian, "Bending behavior of 3D printed sandwich beams with different core topologies," *Mater. Des. Process. Commun.*, vol. 3, no. 4, pp. 1–8, 2021, doi: 10.1002/mdp2.252.

[17] D. Betts, P. Sadeghian, and A. Fam, "Experiments and nonlinear analysis of the impact behaviour of sandwich panels constructed with flax fibre-reinforced polymer faces and foam cores," *J. Sandw. Struct. Mater.*, vol. 23, no. 7, pp. 3139–3163, May 2020, doi: 10.1177/1099636220925073.

[18] E. Labans, K. Kalnins, and C. Bisagni, "Flexural behavior of sandwich panels with cellular wood, plywood stiffener/foam and thermoplastic composite core," *J. Sandw. Struct. Mater.*, vol. 21, no. 2, pp. 784–805, Mar. 2017, doi: 10.1177/1099636217699587.

[19] X. Gao, M. Zhang, Y. Huang, L. Sang, and W. Hou, "Experimental and numerical investigation of thermoplastic honeycomb sandwich structures under bending loading," *Thin-Walled Struct.*, vol. 155, p. 106961, 2020, doi: https://doi.org/10.1016/j.tws.2020.106961.

[20] P. R. Oliveira, M. May, T. H. Panzera, and S. Hiermaier, "Bio-based/green sandwich structures: A review," *Thin-Walled Struct.*, vol. 177, p. 109426, 2022, doi: https://doi.org/10.1016/j.tws.2022.109426.

[21] R. A. Kassab and P. Sadeghian, "Sustainable sandwich composites made of recycled plastics ," *8th International Conference on Structural Engineering, Mechanics and Computation, SEMC 2022* . CRC Press/Balkema , pp. 1509-1514 BT-Current Perspectives and New Dire, 2023, doi: 10.1201/9781003348443-246 .

[22] B. Ravindran, M. Feuchter, and R. Schledjewski, "Investigation of the Mechanical Properties of Sandwich Composite Panels Made with Recyclates and Flax Fiber/Bio-Based Epoxy Processed by Liquid Composite Molding," *Journal of Composites Science*, vol. 7, no. 3. 2023, doi: 10.3390/jcs7030122.

[23] E. Kormaníková and K. Kotrasová, "Dynamic behavior of composite sandwich panel with CFRP outer layers," *WSEAS Trans. Appl. Theor. Mech.*, vol. 17, pp. 263–269, 2022, doi: 10.37394/232011.2022.17.32.

[24] R. Beigpour, H. Shokrollahi, and S. M. R. Khalili, "Experimental and numerical analysis of a biodegradable hybrid

composite under tensile and three-point bending tests," *Compos. Struct.*, vol. 273, no. June, p. 114255, 2021, doi: 10.1016/j.compstruct.2021.114255.

[25] R. Beigpour, S. M. R. Khalili, and H. Shokrollahi, "Lightweight biodegradable hybrid composite sandwich panel under three-point bending loads—Experimental and numerical," *Polym. Compos.*, vol. 43, no. 11, pp. 8007–8029, 2022, doi: 10.1002/pc.26944.

[26] H. C. Cheng, F. Scarpa, T. H. Panzera, I. Farrow, and H. X. Peng, "Shear Stiffness and Energy Absorption of Auxetic Open Cell Foams as Sandwich Cores," *Phys. Status Solidi Basic Res.*, vol. 256, no. 1, pp. 1–9, 2019, doi: 10.1002/pssb.201800411.

[27] C. Kaboğlu, "Investigation of Sandwich Composites with Auxetic Core under Static Loading," *El-Cezeri J. Sci. Eng.*, vol. 9, no. 1, pp. 350–359, 2022, doi: 10.31202/ecjse.978310.

[28] W. Harizi, J. Anjoul, V. A. Acosta Santamaría, Z. Aboura, and V. Briand, "Mechanical behavior of carbon-reinforced thermoplastic sandwich composites with several core types during three-point bending tests," *Compos. Struct.*, vol. 262, no. October 2020, p. 113590, 2021, doi: 10.1016/j.compstruct.2021.113590.